Photoelectron spectroscopic study of the valence and core-level electronic structure of $BaTiO_3$

L. T. Hudson, R. L. Kurtz,* and S. W. Robey
National Institute of Standards and Technology, Gaithersburg, Maryland 20899

D. Temple and R. L. Stockbauer
Department of Physics and Astronomy, Louisiana State University, Baton Rouge, Louisiana 70803
(Received 6 July 1992)

We present valence and core-level photoemission measurements from vacuum-fractured, single-crystal barium titanate. These results resolve contradictory measurements in the literature which have employed other methods of sample surface preparation. The valence-shell electronic structure is compared with previously published results of band structure and cluster calculations. Resonant photoemission is used to probe the covalent coupling between titanium and oxygen in the cubic and tetragonal phases of this ionic compound. Photoelectron spectra of the Ti $2p$ and O $1s$ core levels reveal the valence of these two ions to be TiO_2-like. Valence, core, satellite, and Auger transitions are also assigned and tabulated.

I. INTRODUCTION

The past decade has seen a resurgence of interest in barium titanate because of its favorable performance in fast nonlinear optics applications. In particular, it has become the material of choice in applications requiring large four-wave mixing reflectivity (e.g., phase conjugate resonators) and large beam-coupling gain.[1] The displacive nature of the cubic-to-tetragonal ferroelectric phase transition gives rise to uniaxial optical and dielectric behavior, which in turn determines photorefractive performance. Despite intense study, fundamental questions remain unanswered. Of particular interest in the present work are the details of the electronic structure and the character of the chemical bonding in $BaTiO_3$, both of which are closely linked to the interesting optical and physical properties of this material.

X-ray photoelectron spectroscopic (XPS) studies of $BaTiO_3$ have been performed on ceramic[2,3] and single-crystal[4] $BaTiO_3$ which had been annealed, sputtered, or scraped in air. The only ultraviolet photoemission (UPS) studies have employed sputtered and annealed single crystals.[5,6] These preparation techniques are not entirely satisfactory. Scraping in air does not produce a clean surface; *in situ* scraping creates surface micrograins that react readily with vacuum gases producing additional cationic chemical states.[4] It has been shown that sputtering of $BaTiO_3$ produces a nonstoichiometric surface selvage[2,4–6] and that high-temperature annealing of both sputtered[6] or unsputtered[7] samples introduces new surface phases. We present valence and core-level photoemission studies of vacuum-fractured, single-crystal $BaTiO_3$. In this paper we compare and contrast the measured electronic structure with previously published experiments and calculations and discuss resonant photoemission of the valence band, charge-transfer satellites, valence-band Auger emission, and the importance of covalency effects.

II. EXPERIMENTAL DETAILS

The UPS measurements were performed using the National Institute of Standards and Technology SURF-II synchrotron light source. These measurements employed photons in the energy range of 30–130 eV delivered by a 3-m toroidal grating monochromator. The light was incident at 45° to the surface normal. Angle-integrated spectra were obtained with the sample normal at 45° from the axis of a double-pass cylindrical-mirror analyzer (CMA) operated at a pass energy of 15 eV; the spectra have been normalized to incident photon flux. The overall resolution was a function of photon energy and was about 0.4 eV at $h\nu=38$ eV increasing to about 1 eV at the highest uv photon energies used here. The energy distribution curves (EDC's) are referenced from the common Fermi level (E_F) of the target-detector system as determined by a gold foil which had been cleaned by Ar-ion sputtering. XPS spectra were recorded using an Al $K\alpha$ (1486.6 eV) source with an instrumental resolution of ≈ 1 eV; XPS binding energies were referenced to Au $4f_{7/2} \equiv 84.0$ eV.[8] Uncertainties in peak positions quoted in this paper are estimated to be ≤ 0.2 eV.

The single-crystal $BaTiO_3$ samples used in this study were grown at Louisiana State University using the top-seeded solution-growth technique. When polished, they were a light transparent yellow. The samples were oriented by x-ray diffraction and cut into rectangular rods with faces normal to the [100] family of axes in the cubic system. Our samples were found to charge excessively under the high proton fluxes of the synchrotron light source. This was overcome by chemically reducing the sample by heating *in vacuo*, producing an n-type material. Heating at 900 K for 5 min produced a sample that was a dark, translucent yellow, which charged to a few volts at room temperature as determined by energy shifts of the EDC's. These samples did not charge at elevated temperatures (e.g., 360 K). Higher-temperature

annealing (up to about 1200 K) caused the samples to become increasingly opaque. Under photon irradiation, these severely reduced samples did not charge even at room temperature. From detailed reduction studies of $BaTiO_3$,[9] it is estimated that the moderately reduced (900 K) samples used in this study contained a carrier concentration of $\approx 10^{17}$ electrons/cm^3. The only measurable effect of this reduction on the electronic structure as measured by photoemission is the pinning of the Fermi level at the bottom of the conduction band; indeed, the shapes of the EDC's were found to be independent of the degree of reduction within the range explored. Binding energies quoted in this paper are referenced to this pinned Fermi level. As mentioned above, annealing can create new surface microphases that contribute additional features to photoemission spectra. Accordingly, the samples of this study were fractured *in vacuo* after reduction, generally yielding multifaceted faces with facet normals within a few degrees of the [100] axis.

III. VALENCE ELECTRONIC STRUCTURE OF $BaTiO_3$

Figure 1 shows the EDC's from a vacuum-fractured (100) surface of barium titanate using photon energies of 38 and 46 eV (off and on resonance as discussed below). The sample temperature was 400 K. Also shown are fits to the inelastic background. This background was assumed to be a function proportional to the integrated number of unscattered electrons with higher kinetic energy plus terms linear and quadratic in binding energy. The broad feature from about 13 to 18 eV binding energy is composed of two overlapping, spin-orbit-split doublets due to Ba 5*p* states: a pair due to undercoordinated barium at the surface and a pair due to bulk coordination. A detailed discussion of the spectroscopy of Ba core levels is planned to be considered in a forthcoming publication.[10] The dramatic change in intensity of the Ba 5*p* peaks in these two spectra is consistent with the rapid falloff of the Ba 5*p* atomic photoionization cross section in this energy range.[11] In addition, the $h\nu=38$ eV spectrum includes some small amount of intensity in the Ba 5*p* region due to excitations from Ba 4*d* states by third-order light.

The valence band extends from about 3 to 9 eV below E_F and is derived primarily from O 2*p* states. We determine the position of the valence-band maximum (VBM) by extrapolating the steepest rise of the high-kinetic-energy edge ($h\nu=38$ eV, off resonance as discussed below) to zero. This derived value is about 3.3 eV, which is the width of the optical band gap of $BaTiO_3$.[12] Since E_F presumably resides at the bottom of the Ti 3*d* conduction band in the bulk electronic structure of a reduced sample, we observe negligible band bending on these vacuum-fractured surfaces.

Resonant photoemission can be used to isolate the hybridized titanium-ligand states of the valence band. Excitations from Ti 3*p* to empty Ti 3*d* states can deexcite via direct recombination (or autoionization) and emission of a VB electron. Since direct Ti 3*d* photoemission results in identical initial and final states, these two pathways produce quantum interference.[13] Such resonant emission can be seen in the inset of Fig. 1, which shows the valence band, with inelastic background subtracted, for photon energies below and above the Ti $3p \rightarrow 3d$ optical-absorption transition. The resonance is manifest in the bottom parts of the band; the small decrease of intensity in the top part of the valence band follows the trend of the O 2*p* photoionization cross section. In Fig. 2 the integrated intensity of the valence band above background is shown for spectra taken at incident photon energies of 30–60 eV (black dots). The line through the dots is a guide to the eye for this excitation function. The exact onset is obscured by an experimental artifact. The 4-eV-wide feature centered at 42 eV is caused by Ba 4*d* peaks, produced by third-order light, passing through the window of integration. It is clear, however, that the onset of the resonance is delayed from the Ti 3*p* edge (marked in Fig. 2); we measure the Ti 3*p* binding energy in $BaTiO_3$ to

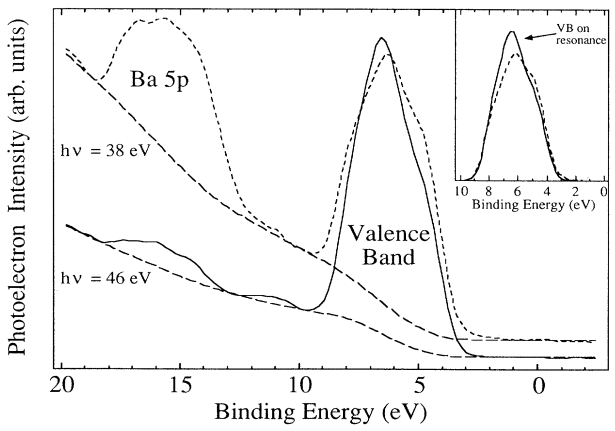

FIG. 1. UPS spectra of vacuum-fractured $BaTiO_3$ (100) at $h\nu=38$ and 46 eV. The inset shows a comparison of valence-shell electronic structure after subtraction of an inelastic background. The binding energy is referenced from $E_F \equiv 0$.

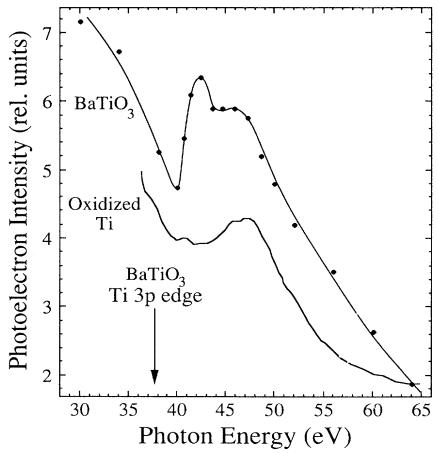

FIG. 2. Resonant photoemission intensity of the oxygen valence band of $BaTiO_3$ as the photon energy is swept through the Ti $3p \rightarrow 3d$ optical-absorption transition. The line through the dots is shown as a guide for the eye. For comparison, the profile from oxidized titanium taken from Ref. 15 is also shown.

be 37.7 eV. The resonance itself is peaked between 46 and 47 eV and continues beyond 64 eV.

This observation of the Ti $3p \rightarrow 3d$ resonance in photoemission of $BaTiO_3$ was anticipated from similar studies of clean and oxidized Ti,[13,14] TiO_2,[15,16] Ti_2O_3,[17] and $SrTiO_3$.[18] For comparison, a previous measurement of this resonance taken in this laboratory[14] from oxidized titanium is also shown in Fig. 2. Resonant $3p \rightarrow 3d$ behavior is also observed in heavier $3d$ transition metals and their compounds. In these systems the profile of the resonance is found to be only a few electron volts in width and well described by a Fano function. $BaTiO_3$ exhibits resonant behavior characteristic of the lighter $3d$ transition metals and their compounds: an onset delayed above the Ti $3p$ edge, which is the expected threshold in a simple, one-electron picture, a profile that is not well described by a Fano function, and a width of tens of electron volts. These differences from the Fano formalism are not fully understood at present. The large width of the resonant profiles has been attributed to multielectron losses.[13]

It is interesting to compare the change in photoemitted O $2p$-VB intensity for various titanium oxides as the photon energy is swept through the Ti $3p$ edge. For $BaTiO_3$ and $SrTiO_3$,[18] an intensity change of approximately 25% is found; the corresponding changes for oxidized Ti,[14] TiO_2 (110),[16] and Ti_2O_3 (Ref. 17) are about 16%, 66%, and 100%, respectively. Smith and Henrich[17] have pointed out, however, the possibility of strong angular anisotropy in the cation $3d$ resonant emission which is related to the molecular-orbital structure of these oxides. Comparisons of the "strength" of resonant behavior from single-crystalline materials using pseudo-angle-integrating CMA's can, therefore, be problematic and difficult to interpret.

Although questions remain as to the detailed nature of the resonant effects, this behavior indicates a significant degree of covalent character in the Ti $3d-$O $2p$ bonding in $BaTiO_3$ even though this material is formally a maximal-valent oxide. Indeed, the very observation of "interatomic" resonant photoemission implies communication between the ions. This is of interest from the point of view of the ferroelectric-to-paraelectric phase transition which occurs at ≈ 400 K in $BaTiO_3$ because the covalent character has been predicted to be an important driver of the ferroelectric instability in this system.[19]

Above its Curie temperature, barium titanate has the cubic perovskite structure which is best visualized by placing Ba in the center of a cube coordinated by 12 oxygens on the cube edges. Titanium ions on the cube corners are sixfold coordinated by oxygen. Below about 400 K, $BaTiO_3$ relaxes to lower-symmetry structures. At room temperature it is tetragonal with a local spontaneous polarization arising predominantly from a 0.13-Å displacement of titanium ions with respect to the centers of their oxygen octahedra.[20] This displacement occurs along the [100] family of axes in the cubic system. Reflectivity spectra[21] and band-structure calculations[22] show that this cubic-to-tetragonal transition is accompanied by changes in energy levels of only 10–150 meV. Because the observed resonant effects are connected to the covalent nature of the Ti-O bonding, we attempted to see if a concomitant change in hybridization might occur which could be observed as a change in the strength of the VB resonant photoemission on going through the cubic-to-tetragonal phase transition. To this end, samples were poled (aligned in the tetragonal phase) by cooling from above T_c to room temperature in a coercive electric field of 1 kV/cm. However, no detectable change in the resonance behavior between the paraelectric and ferroelectric phases was observed.

We now compare our measurement of the valence electronic structure with previous experimental and theoretical studies. The off-resonance ($h\nu = 38$ eV) valence band of Fig. 1 is reproduced in Fig. 3(a) on a binding-energy scale such that the VBM$\equiv$0 eV. The data are unsmoothed and the inelastic background has been subtracted. To help determine the energies of the three obvious components which are also predicted by band-structure calculations, the data (dots) were fit to the sum of three Gaussian functions (solid line). While this decomposition is not unique (intensity could be shifted somewhat between the three peaks, producing compara-

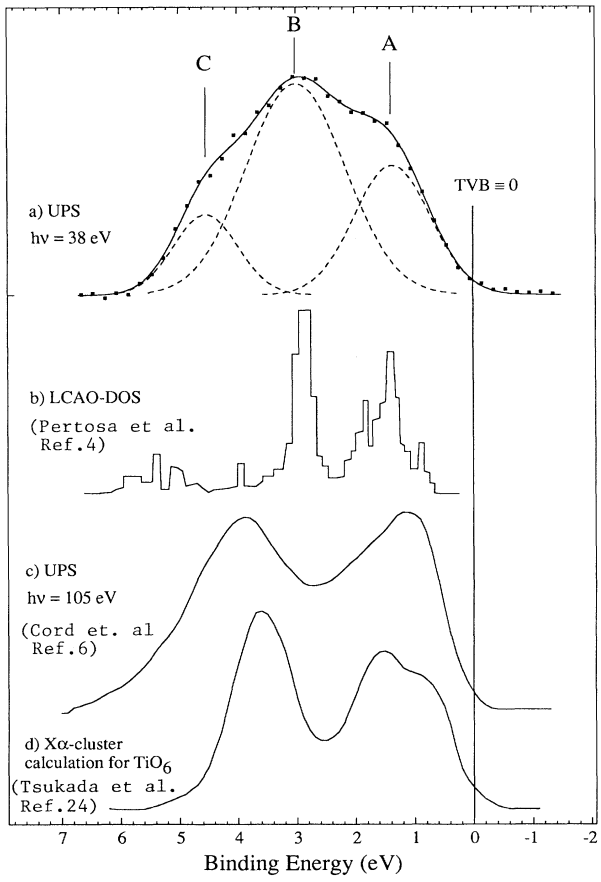

FIG. 3. Valence electronic structure of $BaTiO_3$. The binding energy is referenced from VBM$\equiv$0. (a) Data reproduced from the inset of Fig. 1 ($h\nu = 38$ eV). (b) Density of states histogram from band-structure calculation of Ref. 4. (c) Measurement from sputtered and annealed $BaTiO_3$ from Ref. 6. (d) Calculation for a TiO_6 cluster from Ref. 23.

ble fits to the data), peak positions agreed to within ±0.1 eV. The features marked *A*, *B*, and *C* are centered at binding energies 1.4, 3.0, and 4.5 eV, respectively. Band-structure calculations of cubic $BaTiO_3$ associate peak *A* with nearly pure oxygen states, while peaks *B* and *C* contain O $2p$–Ti $3d$ mixed states.[4,23] This weighting is clearly borne out by the spectra in the inset of Fig. 1. Here the bottom part of the oxygen valence band is enhanced relative to the top as the photon energy is swept past the Ti $3p$ absorption edge.

The band structure of cubic $BaTiO_3$ was calculated in Ref. 4 using a tight-binding, linear combination of atomic orbitals (LCAO) method; the resulting VB density-of-states (DOS) histogram (neglecting inner Ba and Ti orbitals) is shown in Fig. 3(b). The spacing between the centroids of the features corresponding to *A* and *B* (≈ 1.4 eV) agrees quite well with that of the experimental VB of Fig. 3(a) (≈ 1.6 eV). Peak *C*, however, which depends mainly on the value of the $pd\sigma$ interaction, falls about 0.9 eV lower in binding energy in the UPS measurement than in the calculation. While there are different cross-section variations for the states of different symmetry, the spacing of these three UPS-VB features as well as the 5.8-eV bandwidth of Fig. 3(a) agree favorably with early XPS measurements,[2–4] affirming that even with less than ideal surface preparation these XPS measurements of the VB were sufficiently bulk sensitive. As discussed below, there is, however, considerable disagreement with the most recent UPS measurements[6] of the VB electronic structure of $BaTiO_3$.

In work by Cord and Courths,[6] sputtered $BaTiO_3$ was annealed at 1200 K, producing new features in UPS ($h\nu = 105$ eV) spectra. These were ascribed to stoichiometric, bulk $BaTiO_3$, and the appropriate difference spectrum generated the two-peaked VB shown in Fig. 3(c). The spacing between the two features is 2.7 eV, which was compared in Ref. 6 with the results of an $X\alpha$-cluster calculation[24] of a bulk $(TiO_6)^{8-}$ cluster [Fig. 3(d)]. While some of our vacuum fractures produced a valence electronic structure in which features *A* and *B* appeared more resolved than that of Fig. 3(a), the spacing between the features *A* and *B* was always ≈ 1.6 eV. It has been pointed out[25] that tight-binding computations are more adapted to reproduce the electronic structure of perovskite materials. Both the finite cluster size and the muffin-tin approximation of $X\alpha$-cluster calculations lead to bandwidths that are too narrow. Furthermore, the high-binding-energy tail (feature *C*) is missing in the $X\alpha$ DOS since cluster calculations retain only the main symmetry points of the Brillouin zone.[26] We propose that the data of Fig. 3(c) represent not bulk $BaTiO_3$, but a surface microphase produced by harsh annealing of the sample. Recent work has shown that reduction at 1650 K produces surface compositions that are close to Ba_2TiO_4.[7] Here the main structural motif is the TiO_4 tetrahedron rather than the TiO_6 octahedron of $BaTiO_3$. Accordingly, the VB electronic structure of a surface-sensitive UPS measurement would be greatly affected. An earlier UPS study[5] in which ion-bombarded samples were annealed to only 970 K gave results more in agreement with the present work.

IV. AUGER AND CORE-LEVEL PHOTOELECTRON SPECTROSCOPY OF $BaTiO_3$

The shallow core levels of cubic $BaTiO_3$ (sample temperature = 440 K) are revealed by $h\nu = 130$ eV excitation in Fig. 4. Similar results were found for tetragonal $BaTiO_3$ at room temperature. The peak positions (and assignments), listed in Table I, were determined by subtracting an inelastic background and fitting each peak with a Gaussian function. For the barium levels, the centroid of the unresolved emission is tabulated.

The two broad features at binding energies (BE's) 74.7 and 61.4 eV in Fig. 4 were found to remain at constant kinetic energies as the incident photon energy was varied. These are identified as barium Auger peaks since the Ba $4d$ levels are the only core levels reached by 130-eV photons that could result in the observed kinetic energies as high as $h\nu - \mathrm{BE} = 55.3$ and 68.6 eV with respect to E_F (there is no higher-order light at this monochromator setting). The kinetic energy of an Auger electron with respect to the Fermi level can be written as $E(a) - E(b) - E(c) - U_{\mathrm{eff}}$. Here the *E*'s are the binding energies of the states involved: the initial core hole *a*, which is filled by electron *b* with the ejection of electron *c*. U_{eff}, the effective core-hole potential, is the Coulomb repulsion energy of the two-hole final state modified by the relaxation energy. The observed kinetic energies are too high to be $N_{45}OO$ or $N_{45}OO_{23}$ transitions, and the higher-kinetic-energy Auger peak is too energetic to be $N_{45}O_{23}O_{23}$. This higher-energy peak then must be $N_{45}O_{23}V$ (i.e., *a* = Ba $4d$, *b* = Ba $5p$, and *c* = valence band) or $N_{45}VV$; the latter is less probable since, depending on

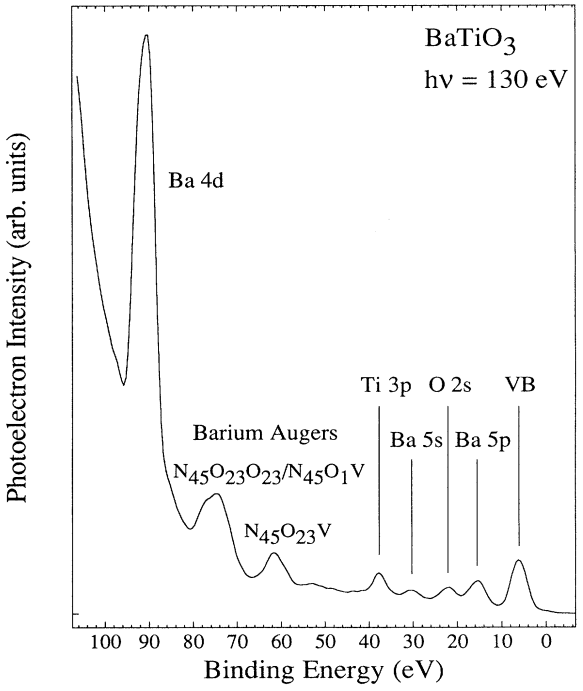

FIG. 4. Photoelectron spectrum of the shallow core levels of $BaTiO_3$. $h\nu = 130$ eV.

TABLE I. UPS and XPS binding energies for vacuum-fractured $BaTiO_3$ from spectra of Figs. 3–6.

Level	Binding energy (±0.2 eV) ($E_F \equiv 0$)	Photon energy (eV)
VB feature *A*	4.7	38
VB feature *B*	6.3	38
VB feature *C*	7.8	38
Ba 5*p*	15.5	130
O 2*s*	22.1	130
Ba 5*s*	30.3	130
Ti 3*p*	37.7	130
Ba $N_{45}O_{23}O_{23}$ and/or $N_{45}O_1V$ Auger	55.3 (kinetic energy)	130
Ba $N_{45}O_{23}V$ Auger	68.6 (kinetic energy)	130
Ba 4*d*	90.9	130
Ti $2p\ \frac{3}{2}$	459.0	1487
Ti $2p\ \frac{3}{2}$ satellite	472.1	1487
Ti $2p\ \frac{1}{2}$	464.6	1487
Ti $2p\ \frac{1}{2}$ satellite	477.6	1487
O 1*s*	530.3	1487

the particular valence-band levels participating it would require a $U_{\text{eff}} \approx 7-13$ eV, which is larger than expected for hole-hole repulsion in a relatively delocalized VB and for a peak so broad. In a study of electron-induced, low-energy Auger emission from BaO,[27] the Ba $N_{45}VV$ transition was about 11 eV above the $N_{45}O_{23}V$ peak and much less intense. It was found to have a kinetic energy of 79 eV, which would place it at a binding-energy position of 51 eV in Fig. 4. The $N_{45}VV$ peak, then, may contribute to the faint structure in this region of the spectrum. Therefore the higher-kinetic-energy Auger peak is assigned to the $N_{45}O_{23}V$ transition. Two possible transitions vie for the lower-kinetic-energy peak assignment. If one assumes a similar U_{eff} value for the analogous barium Auger transitions of BaO and $BaTiO_3$ (in BaO U_{eff} is positive and ≤ 1.5 eV), then the lower-kinetic-energy Auger peak is identified as $N_{45}OV$. If U_{eff} is > 1.5 eV, then $N_{45}O_{23}O_{23}$ is also a viable assignment. This lower-kinetic-energy Auger line shape is significantly broader than the higher-energy Auger peak and could possibly contain both of these transitions. We therefore assign the lower-kinetic-energy Auger peak to the $N_{45}O_{23}O_{23}/N_{45}OV$ transition(s). From these assignments we estimate U_{eff} associated with the $N_{45}O_{23}O_{23}$ Auger peak to be about 4.6 eV; the corresponding range of values of U_{eff} for the $N_{45}OV$ and $N_{45}O_{23}V$ transitions are -2.5–0.6 and -1.0–2.1 eV, respectively. The requirement that the high-energy Auger electron transition involve a VB electron provides another example of covalency in barium titanate and, in this case, points toward the non-negligible barium character that has been predicted to increase the Ti-O covalency within the valence band of this compound.[28] Ba-O hybridization is not thought to be very large, however, since we did not observe a strong, reproducible resonance of the O 2*p* VB as the incident photon energy was swept through the so-called "giant" Ba $4d \rightarrow 4f$ resonance. This difference between titanium and barium bonding with oxygen is due to the symmetry of the cation valence electrons (*d*-*p* bonding vs *s*-*p*) and the relatively large electronegativity of titanium.

The oxygen 1*s* and titanium 2*p* core levels from vacuum-fractured $BaTiO_3$ are shown in Figs. 5 and 6, and the centroids of Gaussian fits to the main lines and satellites are recorded in Table I. These data are unsmoothed and were obtained with Al $K\alpha$ excitation. In the measurement of the O 1*s* peak of $BaTiO_3$ at room temperature (Fig. 5), a high-binding-energy shoulder was observed about 2 eV above the main peak and is attributed to adsorption of vacuum gases; it is easily removed by heating the sample to ≥ 520 K. This impurity feature was also noted in a previous study of ceramic barium titanate.[2] In the tetragonal phase, there are two nonequivalent oxygen sites, but a core-level shift of energy levels due to this change in topology is expected from theoretical calculations[20] to result in O 1*s* levels separated from each other by much less than an electron volt. None of the other Ba or Ti XPS line shapes or binding energies were observed to change as a function of sample temperature. The intrinsic O 1*s* level is found to be at 530.3 eV

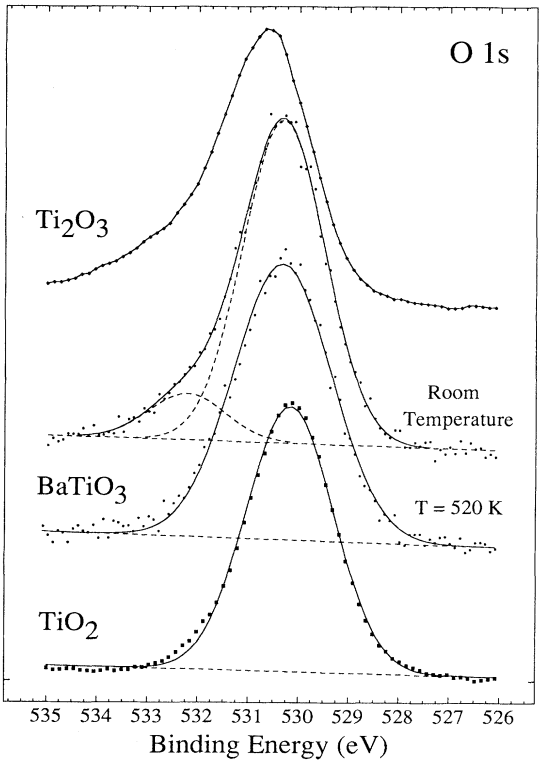

FIG. 5. Comparison of the XPS spectra of O 1*s* core levels from vacuum-fractured Ti_2O_3, vacuum-fractured $BaTiO_3$, and TiO_2 which had been sputtered and annealed. The room-temperature line shape from $BaTiO_3$ (and Ti_2O_3) exhibits a high-binding-energy shoulder due to adsorbed vacuum gases. This feature is easily removed by heating to 520 K.

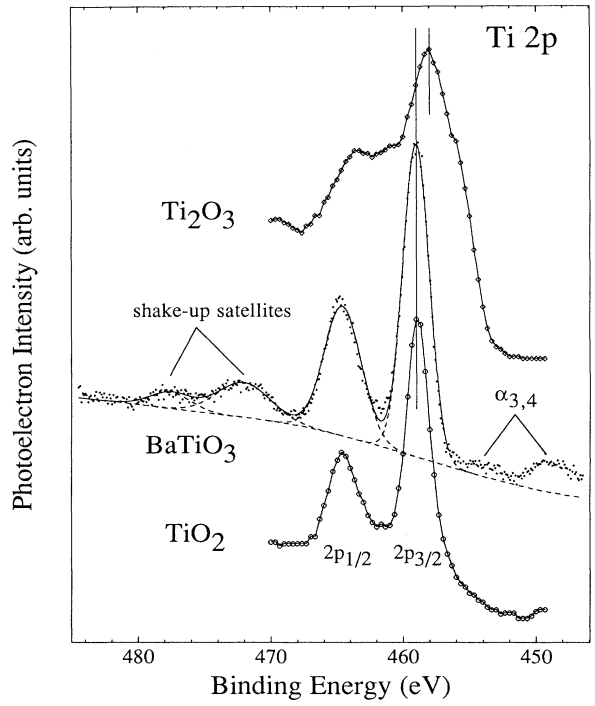

FIG. 6. Comparison of the XPS spectra of Ti 2*p* core levels from vacuum-fractured Ti_2O_3, vacuum-fractured $BaTiO_3$, and TiO_2 which had been sputtered and annealed.

binding energy. For comparison, previously unpublished measurements from vacuum-fractured Ti_2O_3 and TiO_2 which had been sputtered and annealed (the "recipe" for producing a stoichiometric surface in this system) are shown in Figs. 5 and 6. The line shape from Ti_2O_3 possesses the high-binding-energy shoulder exhibited by the room-temperature line shape of $BaTiO_3$ and may also be due to contamination. The O 1*s* levels in $BaTiO_3$ and TiO_2 are similar to binding energy and line shape to within experimental uncertainty.

In the room-temperature spectrum of the Ti 2*p* levels of $BaTiO_3$ (Fig. 6), the features labeled $\alpha_{3,4}$ are due to the satellite Al $K\alpha_{3,4}$ lines from the x-ray source. The high-binding-energy satellites in Fig. 6 are each 13.0 eV above their respective spin-orbit component. Such satellites are often observed to accompany *L*-shell photoelectron lines in 3*d* transition-metal compounds such as the titanium fluorides,[29] TiO_2,[29] and $SrTiO_3$.[30] The energy-loss function of $BaTiO_3$, derived from optical constants,[31] exhibits a feature of 13 eV (and another at 27 eV associated with plasmon energy losses, which are manifest as satellites in our Ba 3*d* XPS spectra). Extrinsic processes, however, can account for only a few percent of the Ti 2*p* satellite intensity based on energy-loss intensity below other core-level peaks of $BaTiO_3$. The Ti 2*p* satellites also cannot be assigned to core–to–conduction-band transitions which have a threshold at 14.4 eV.[32] Since these satellites are observed to depend on the nature of the ligand and are not observed in the metals or in compounds of metals that have filled *d* bands, they have often been associated with shake-up transitions of the charge-transfer type, i.e., ligand valence orbitals to empty 3*d* orbitals of the metal ion. Based upon monopole selection rules, overlap integrals, and energetics arguments, Kim and Winograd[30] assigned the analogous shake-up satellites in isoelectronic $SrTiO_3$ (separated from the main Ti 2*p* peaks by about 13.6 eV) to $2p\sigma e_g \rightarrow 3de_g$. This same transition has also been assigned to the Ti 2*p* satellites of barium titanate.[33] More recently, however, it has been argued that in the early transition-metal compounds an exciton satellite mechanism dominates charge transfer. In the barium titanate system, this model predicts that energy is lost in the creation of an anionic exciton: O $2p \rightarrow$ O $3s$.[34]

The line shape of the Ti 2*p* core levels from Ti_2O_3 differs considerably from the other two line shapes in Fig. 6. Ti_2O_3 exhibits multiple unresolved Ti 2*p* components attributed to well-screened and poorly screened core holes.[35] (A similar Ti 2*p* line shape is observed after sputtering TiO_2.) The highest-binding-energy 2*p* components (poorly screened final states) in Ti_2O_3 are located $\sim$1 eV lower in binding energy than the Ti 2*p* levels in TiO_2 and $BaTiO_3$, however. This positive, initial-state chemical shift is expected since the *formal* oxidation state in Ti_2O_3 is 3+, while it is 4+ in the other two maximal-valence materials.

Since the O 1*s* and Ti 2*p* core levels in $BaTiO_3$ and TiO_2 have identical binding energies and line shapes, we infer that the Ti oxidation state is very similar in these two materials. Recent calculations[19] indicate that ferroelectricity in $BaTiO_3$ originates in a charge-density distortion around the Ti cation rather than the O ligand. For this to occur, a significant Ti-O hybridization is required, and as a result, the effective charge on the Ti was predicted to be reduced to $Ti^{2.9+}$. We would then expect a similar reduction from formal valence to exist in TiO_2. We know TiO_2 is not a completely ionic material since, as discussed above, Ti photoemission resonances have been observed in the valence band of this material as well.[16,17] Indeed, calculations[36] indicate a non-negligible Ti contribution to the valence bands and a Raman-spectroscopic study[37] infers a reduced Ti-O ionicity comparable to that quoted above for $BaTiO_3$. These observations and our measurements imply that the degree of Ti-O covalency in $BaTiO_3$ is similar to that in TiO_2 and that the titanium valence is significantly reduced from 4+ in these materials. That the strength of the titanium resonance in the oxygen valence bands differs in these two materials may be attributed to the problems discussed above, which are inherent in comparing these strengths.

V. CONCLUSIONS

We have presented photoelectron spectra of the electronic structure of barium titanate. After a review of previous photoemission measurements, we conclude that cleaving in vacuum is the preferred method of sample preparation to produce an unobscured view of the bulk electronic structure of $BaTiO_3$. The measured valence-shell structure is better represented by the results of LCAO band-structure calculations[4] than $X\alpha$-cluster cal-

culations.[24] The electronic structure and resonant photoemission behavior was found to be not significantly affected by the cubic-to-tetragonal phase transition of $BaTiO_3$. Based on the resonant photoemission results and core-level measurements, the Ti-O covalency is found to be very similar in $BaTiO_3$ and TiO_2 and consistent with the prediction[19] that the static charges in $BaTiO_3$ are greatly reduced from the formal valence. Along with the resonant photoemission results, barium Auger emission involving the valence band provides another example of covalency effects in the valence band of this material.

ACKNOWLEDGMENTS

The authors gratefully acknowledge the assistance and technical support of the staff of the NIST SURF-II synchrotron. One of us (L.T.H.) expresses appreciation for financial support from the NIST.

*Present address: Department of Physics and Astronomy, Louisiana State University, Baton Rouge, LA 70803.

[1]M. B. Klein, in *Photorefractive Materials and Their Applications I,* Vol. 61 of *Topics in Applied Physics,* edited by P. Günter and J.-P. Huignard (Springer-Verlag, Berlin, 1988), p. 195.

[2]F. L. Battye, H. Höchst, and A. Goldmann, Solid State Commun. **19**, 269 (1976).

[3]H. Nakamatsu, H. Adachi, and S. Ikeda, J. Electron Spectrosc. Relat. Phenom. **24**, 149 (1981).

[4]P. Pertosa and F. M. Michel-Calendini, Phys. Rev. B **17**, 2011 (1978).

[5]R. Courths, Phys. Status Solidi B **100**, 135 (1980).

[6]B. Cord and R. Courths, Surf. Sci. **152-153**, 1141 (1985).

[7]B. B. Leikina, M. A. Kvantov, and Yu. P. Kostikov, Izv. Akad. Nauk SSSR Neorg. Mater. **16**, 135 (1990).

[8]P. H. Citrin, G. K. Wertheim, and Y. Baer, Phys. Rev. Lett. **41**, 1425 (1978).

[9]J. Dubuisson and P. Basseville, in *The Role of Grain Boundaries and Surfaces in Ceramics,* Vol. 3 of *Materials Science Research,* edited by W. W. Kriegal and H. Palmour III (Plenum, New York, 1966), p. 77.

[10]L. T. Hudson, R. L. Kurtz, S. W. Robey, D. Temple, and R. L. Stockbauer (unpublished).

[11]J. J. Yeh and I. Lindau, At. Data Nucl. Data Tables **32**, 10 (1985); **32**, 76 (1985).

[12]S. H. Wemple, Phys. Rev. B **7**, 2679 (1970).

[13]J. Barth, G. Gerkin, and C. Kunz, Phys. Rev. B **31**, 2022 (1985).

[14]E. Bertel, R. Stockbauer, and T. E. Madey, Phys. Rev. B **27**, 1939 (1983); E. Bertel, R. Stockbauer, and T. E. Madey, Surf. Sci. **141**, 355 (1984).

[15]R. L. Kurtz, R. Stockbauer, and T. E. Madey, in *Desorption Induced by Electronic Transitions-DIET II,* edited by W. Brenig and D. Menzel (Springer, New York, 1985), p. 89.

[16]Z. Zhang, S. Jeng, and V. E. Henrich, Phys. Rev. B **43**, 12 004 (1991).

[17]K. E. Smith and V. E. Henrich, Phys. Rev. B **38**, 9571 (1985).

[18]N. B. Brookes, D. S.-L. Law, T. S. Padmore, D. R. Warburton, and G. Thornton, Solid State Commun. **57**, 473 (1986).

[19]R. E. Cohen and H. Krakauer, Phys. Rev. B **42**, 6416 (1990).

[20]H. D. Megaw, *Ferroelectricity in Crystals* (Methuen, London, 1957), p. 62.

[21]M. Cardona, Phys. Rev. **140**, A651 (1965); D. Bäuerle, W. Braun, V. Saile, G. Sprüssel, and E. E. Koch, Z. Phys. B **29**, 179 (1978).

[22]F. M. Michel-Calendini and G. Mesnard, Phys. Status Solidi **44**, K117 (1971); F. M. Michel-Calendini and G. Mesnard, J. Phys. C **6**, 1709 (1973).

[23]V. R. Marathe, S. Lauer, and A. Trautwein, Phys. Status Solidi B **100**, 149 (1980).

[24]M. Tsukada, C. Satoko, and H. Adachi, J. Phys. Soc. Jpn. **48**, 200 (1980).

[25]L. Castet-Mejean and F. M. Michel-Calendini, Ferroelectrics **37**, 503 (1981).

[26]F. M. Michel-Calendini, H. Chermette, and J. Weber, J. Phys. C **13**, 1427 (1980).

[27]G. A. Haas, C. R. K. Marrian, and A. Shih, Appl. Surf. Sci. **16**, 125 (1983).

[28]V. V. Nemoshkalenko and A. N. Timoshevskii, Phys. Status Solidi B **127**, 163 (1985).

[29]T. A. Carlson, J. C. Carver, L.J. Saethre, F. Santibanez, and G. A. Vernon, J. Electron Spectrosc. Relat. Phenom. **5**, 247 (1974); B. Wallbank, I. G. Main, and C. E. Johnson, *ibid.* **5**, 259 (1974).

[30]K. S. Kim and N. Winograd, Chem. Phys. Lett. **31**, 312 (1975).

[31]M. Cardona, Phys. Rev. **140**, A651 (1965).

[32]D. Bäuerle, W. Braun, V. Saile, G. Sprüssel, and E. E. Koch, Z. Phys. B **29**, 179 (1989).

[33]H. Chermette, P. Pertosa, and F. M. Michel-Calendini, Chem. Phys. Lett. **69**, 240 (1980).

[34]D. K. G. de Boer, C. Haas, and G. A. Sawatzky, Phys. Rev. B **29**, 4401 (1984); J. Park, S. Ryu, M. Han, and S.-J. Oh, Phys. Rev. B **37**, 10 867 (1988).

[35]R. L. Kurtz and V. E. Henrich (unpublished). This mechanism has also been assigned to the Ti $2p$ line shape of $LiTi_2O_4$ in P. P. Edwards, R. G. Egdell, I. Fragala, J. B. Goodenough, M. R. Harrison, A. F. Orchard, and E. G. Scott, J. Solid State Chem. **54**, 127 (1984).

[36]S. Munnix and M. Schmeits, Phys. Rev. B **30**, 2202 (1984).

[37]G. A. Samara and P. S. Peercy, Phys. Rev. B **7**, 1131 (1973).